Accumulation of DOC in the South Pacific Subtropical Gyre from a molecular perspective

Helena Osterholz*, David Kilgour, Dominik Sebastian Storey, Gaute Lavik, Timothy Ferdelman, Jutta Niggemann, Thorsten Dittmar

Author affiliations:
HO, DSS, JN, TD: Marine Geochemistry, ICBM, Carl von Ossietzky University, Oldenburg, Germany
HO: Current affiliation: Marine Chemistry, Institute for Baltic Sea Research, Rostock, Germany
DPAK: Nottingham Trent University, Nottingham, United Kingdom (david.kilgour@ntu.ac.uk)
GL, TF: Biogeochemistry, Max Planck Institute for Marine Microbiology, Bremen, Germany (glavik@mpi-bremen.de, tferdelm@mpi-bremen.de)
TD: HIFMB, Carl von Ossietzky University, Oldenburg, Germany

*corresponding author

Running title: DOM in the South Pacific

Keywords: FT-ICR-MS, ultrahigh-resolution mass spectrometry, solid-phase extraction, molecular formula, subtropical gyre, refractory DOM, photochemistry

Highlights

- DOM concentration and composition were assessed in the South Pacific.
- DOC accumulates in the surface oligotrophic South Pacific Subtropical gyre.
- DOM molecular composition reveals low C/N and imprint of photodegradation.
- Solid-phase extracted DOM fraction suitable to trace DOM ageing across ocean basins.

Abstract

The subtropical South Pacific Gyre (SPG) encompasses the largest oligotrophic region of the global ocean. In these remote waters dissolved organic matter (DOM) accumulates in the surface waters, though constituting a potential source of nutrients and energy to sustain microbial life. On a zonal transect across the SPG, we quantified bulk dissolved organic carbon (DOC) and assessed the DOM composition via ultrahigh resolution mass spectrometry (UHR-MS) of solid-phase extracted DOC (SPE-DOC) to elucidate the molecular-level reasons behind the apparent recalcitrance of the DOM prevailing in the SPG. We included a comparison between two individual formula assignment approaches to UHR-MS data in absorption and magnitude mode which yielded consistent results.

DOC concentrations exceeding 100 µmol C L^{-1} in the warm and saline waters of the central gyre were higher than in the surface waters of the adjacent western South Pacific. Along the transect, concentrations of SPE-DOC were less variable than bulk DOC. Nevertheless, molecular-level investigation revealed that the composition of the DOM accumulated in the central SPG generally conformed to characteristics of surface ocean DOM, but all assessed properties were more pronounced. We found high abundances of potentially labile unsaturated aliphatic molecular formulas and a low calculated degradation index for the DOM of likely marine microbial origin. Markedly decreased molar N/C ratios in the central gyre indicated preferential microbial utilization of nitrogen-containing DOM. A distinct imprint of extensive photochemical reworking was manifested in the low aromaticity of the DOM in the photic layer. Over the whole water column, ageing of DOM was evident through the small, but significant contribution of SPE-DOC to apparent oxygen utilization as well as on molecular level. Our findings demonstrate that SPE-DOC captures carbon fractions relevant on timescales of seasons to timescales covering ocean circulation and biogeochemical processes in stable gyre systems are imprinted in the DOM molecular composition.

Introduction

Dissolved organic carbon (DOC) in the oceans comprises a mixture of organic molecules spanning a wide range of ages, origins and reactivities. Its distribution and composition are controlled by biological and hydrographic processes. Biological production is mostly limited to the sunlit surface waters, while subduction and deep convection processes control deep ocean DOC concentrations (Carlson and Ducklow, 1995; Hansell and Carlson, 1998; Romera-Castillo et al., 2016).

Highest fluxes but at the same time low concentrations of freshly produced, labile DOC can be observed at the production sites; semi-labile species accumulate in the surface ocean, while deep-ocean DOC concentration and composition are relatively uniform. On the other hand, recalcitrant DOM, i.e. forms of DOM not easily accessed and broken down by microbes, is thought to be distributed evenly throughout the water column, in the deep ocean (Hansell, 2013).

In oceanic subtropical gyres, covering more than 60% of the global ocean surface waters (Karl, 2002), dissolved organic matter (DOM) accumulates in the photic layer of the central gyre waters to concentrations often exceeding 70 µmol L^{-1} (Hansell et al., 2009; Raimbault et al., 2008). The South Pacific Gyre (SPG), the largest of the world's oceanic gyre systems, shows the most extreme oligotrophic conditions (Dandonneau et al., 2006): Nitrate-deplete waters with concentration always below 0.01 µmol L^{-1} (Raimbault et al., 2008) lead to year-round low chlorophyll *a* concentrations not exceeding 0.03 µg L^{-1} and the clearest waters (Claustre and Maritorena, 2003) (Morel et al., 2007). CO_2 fixation rates from nitrate-based new production or dinitrogen fixation are low (Raimbault and Garcia, 2008; Shiozaki et al., 2018). An interplay of many factors is hypothesized to contribute to DOM accumulation. Nutrient limitation and associated DOC overproduction have been proposed (Biersmith and Benner, 1998; Thingstad et al., 1997). Along similar lines, Raimbault et al. (2008) suggest that low primary production, restricted by nutrient supply, can lead to the accumulation of C-rich organic matter in the closed ecosystem of the central gyre waters due to weak lateral advection and preferential removal of N- and P-moieties from dissolved organics (Letscher and Moore, 2015). Limited availability of nitrogen, but not iron, and labile carbon sources were previously experimentally identified as impairing heterotrophic growth in the southern Pacific (Van Wambeke et al., 2008). Other studies have attributed the accumulation of semi-labile DOM in surface gyre waters mainly to vertical stratification (Goldberg et al., 2010; Hansell et al., 2009; Skoog and Benner, 1997). On molecular

level, strong solar irradiation of the clear, low latitude waters may produce intrinsically stable DOM compounds via photohumification (Benner and Biddanda, 1998; Obernosterer and Benner, 2003; Obernosterer et al., 1999), leading to an accumulation of recalcitrant DOC. In addition to the intrinsic stability of certain structures in DOM, the high dilution of single compounds below a metabolically profitable threshold or environmental constraints, e.g. through lack of nutrients, have been hypothesized to contribute to the millennial-scale stability in the oceans (Arrieta et al., 2015; Dittmar, 2014; Jiao et al., 2011; Mentges et al., 2019).

DOC in the oceans makes up one of the largest actively cycled carbon pools on earth (Williams and Druffel, 1987). The bulk C concentrations of the DOM pool can be quantified via high temperature catalytic combustion or wet chemical oxidation through detection of CO_2 released from organically bound C (Menzel and Vaccaro, 1964; Ogawa and Ogura, 1992; Sharp et al., 2002). Thus, initial conclusions about reactivity and source of the organic matter can be drawn from distribution of DOC concentrations, if analyzed over spatial or temporal gradients. Few biomolecules are directly recognizable in DOM, of which amino acids and neutral sugars are readily utilized by heterotroph microbes (Jørgensen et al., 2014). Solid-phase extraction (SPE), especially using PPL columns (Dittmar et al., 2008) has become the most commonly applied method to extract and concentrate DOM from water samples for subsequent untargeted mass spectrometric analyses (Green et al., 2014). PPL-SPE is biased against very small and polar molecules and colloids (Perminova et al., 2014; Raeke et al., 2016; Sleighter and Hatcher, 2008), and is considered to be more representative of the recalcitrant DOM pool (Hansman et al., 2015), although it does capture recently produced DOM as well (Wienhausen et al., 2017). Fourier-transform ion cyclotron resonance mass spectrometry (FT-ICR-MS, (Comisarow and Marshall, 1974; Marshall et al., 1998)) of SPE-DOM has become a widely applied approach in marine biogeochemical studies. Across oceans, FT-ICR-MS has successfully been applied to investigate DOM molecular mass; heteroelement content; degree of oxidation or aromaticity; as well as turnover estimates of DOM subpools due to microbial or photochemical processing (Hansman et al., 2015; Landa et al., 2018; Medeiros et al., 2016; Stubbins and Dittmar, 2015). Yet, little is known about the molecular composition of DOM accumulating in subtropical gyres. The high precision and mass accuracy of the FT-ICR-MS allow the assignment of molecular formulas to tens of thousands of compounds in highly complex mixtures (G. Marshall et al., 2013; Kind and Fiehn,

2007; Koch et al., 2005; Smith et al., 2018). Improving the computationally intensive molecular formula attribution process is a field of ongoing research; different approaches can be taken, based on in-house developed routines, or using a variety of free or commercially available programs. In this study, we integrate a comparison between two molecular formula assignment pipelines following FT-ICR-MS data collection (Supplemental Figure S1): For the first approach, the magnitude mode spectrum is analyzed. In magnitude mode, the most widely applied mode of operation in natural organic matter studies (Da Silva et al., 2020), the time-domain data is converted to the frequency domain using the magnitude from the Fourier transformation. A challenge here is that the accuracy of the analysis increases with mass, as does the number of possible assignments. Molecular formulas are then assigned to the accurate masses within a certain error range, making use of spectra alignment, recalibration, and applying several conditions regarding elemental ratios and $\delta^{13}C$ ratios (Merder et al., 2020). In the second approach, the absorption mode processing, the phase of the ions is known and taken into account for the conversion to the frequency domain. This increases the resolving power, mass accuracy and sensitivity (Kilgour et al., 2013), but phase correction must be performed carefully (Kilgour and Van Orden, 2015; Qi et al., 2011). The absorption mode processing is then followed by formulaic assignment by inference, through a network of homologous series, constructed from the mass differences between detected peaks in the mass spectra.

During the SO245 UltraPac expedition (Process oriented biogeochemical, microbiological, and ecological investigations of the ultraoligotrophic South Pacific Gyre), on board the RV Sonne, we passed through the most oligotrophic, central SPG waters (Figure 1). The >8000 km transect from Chile to New Zealand was the first sampling campaign covering the whole South Pacific from East to West since the BIOSOPE cruise in 2004 (Claustre et al., 2008). Along the zonal transect, we examined the basin-wide dissolved organic matter distribution and composition and appraise the value and limitations of captured carbon fractions in context of environmental interpretation to better understand the reasons behind DOM accumulation in the subtropical gyre waters from a molecular point of view. Focusing on the upper water column, we combined FT-ICR-MS-derived heteroelement contributions and structural indices with physical and chemical oceanography to maximize our understanding of DOM cycling in the oligotrophic South Pacific.

Materials and Methods:

Water samples were obtained along a transect from Antofagasta (Chile) to Wellington (New Zealand) on the R/V Sonne cruise SO245 in the austral summer of 2015/2016. Water samples were retrieved from different water depths at 15 stations, alternating between deep (to bottom water, even numbered stations and station 15) and intermediate stations (to 500 m water depth, odd numbered stations, Figure 1), using 12 L Niskin bottles attached to a conductivity, temperature and depth (CTD) probe (Seabird sbe911+, Seabird Scientific, WA, USA). Further details on sensors and underwater light field measurements can be found in Reintjes et al. (2019). Physical oceanography, oxygen and nutrient data are available via the Pangaea database (Ferdelman et al., 2019a; Ferdelman et al., 2019b; Zielinski et al., 2018).

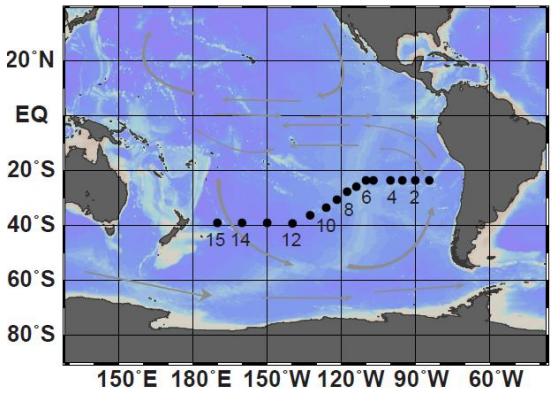

Figure 1 - Cruise track of SO245. Black circles denote sampling stations; deep stations are marked with station numbers. Grey arrows show main ocean currents. Map created with Ocean Data View (Schlitzer, 2018).

Quantification of total dissolved (free and combined, TDNS, hydrolysed 0.1 M HCl, 20 h, 100°C under N_2) and free dissolved neutral sugars (FDNS) was performed at stations 2, 6 and 8, to a maximum of 600 m water depth from 0.2 µm (Acrodisc GHP, Sigma-Aldrich, Inc., USA) filtered water samples. Analyses was performed as described in Mopper et al. (1992) by HPLC with a Carbopac PA1 column (Dionex, Thermo Fisher Scientific Inc., USA) and pulsed amperometric detection. Samples were desalted prior to analysis using ion-exchange resins.

For DOM analyses, four-liter water samples were gravity filtered through 0.7 µm GF/F filters and acidified to pH 2 (HCl). Duplicate subsamples for DOC and total dissolved nitrogen (TDN) were acidified to pH2 and stored at 7°C in the dark in 20 ml glass vials with PTFE septa, and analyzed upon arrival in the home laboratory. A number of additional DOC/TDN samples were filtered through 0.2 µm polycarbonate filters and stored frozen in acid-rinsed 50 mL

polypropylene tubes until analysis. All material used for sampling was precombusted (4 hrs, 400°C; glassware) or thoroughly soaked in ultrapure water at pH2 and rinsed with sample before use. DOC and TDN were analyzed by high temperature catalytic combustion using a TOC-VCPH/CPN Total Organic Carbon Analyzer equipped with an ASI-V autosampler and a TNM-1 module (Shimadzu, Kyoto, Japan). L-arginine solutions ranging from 5 to 500 µmol C/L and 3.3 to 333.3 µmol N/L were used for calibration. Precision and accuracy for DOC and TDN were assessed from repeated analyses of a deep Florida Strait reference material (DSR), provided by D.A. Hansell (University of Miami, Florida, USA), and were better than 5%. If analyses of replicate environmental samples deviated by more than 10%, the sample of higher concentration was removed from the dataset as it was likely a result of contamination during handling or transport. The number of replicates included with DOC and TDN concentrations is provided in the Supplemental Material. Overall, 211 and 272 samples for DOC and TDN, respectively, were obtained across the transect. Dissolved organic nitrogen (DON) concentrations were determined indirectly as the difference between TDN and dissolved inorganic nitrogen from nitrate and nitrite, ammonium data was not available. Ammonium is present only at low nanomolar concentrations in the open ocean and thus does not severely impact the calculation (Gruber, 2008). The analytical error of two different methods is compounded in the DON concentrations and outliers with negative values were removed from the analysis (Graeber et al., 2012).

The remaining volume of the filtered acidified seawater was solid-phase extracted using commercially available modified styrene divinyl benzene copolymer cartridges (1g PPL, Agilent, Santa Clara, CA, USA) as described in Dittmar et al. (2008). Methanol extracts were stored in the dark at -18°C. SPE-DOC and SPE-DON concentrations in the extracts were obtained by drying 1 mL of the methanol extract and redissolution of the dried extract in 10 ml ultrapure water at pH 2 for DOC quantification as described above. The extraction efficiency was 38±8 % on a DOC basis. SPE-DOC concentrations were highly reproducible and deviated by less than 2.1% between replicate extractions that were performed for five samples covering a wide range of depths (Supplemental Table S1).

Before analysis of the DOM molecular composition via FT-ICR-MS, the extracts were diluted to an approximate concentration of 2.5 ppm C in a mixture of methanol and water (1:1 v:v). Direct infusion electrospray ionization (ESI) FT-ICR mass spectra were acquired on a 15 T

Solarix (Bruker Daltonics, Billerica, MA, USA) using a PAL autosampler. The ESI source was heated to 200°C and capillary voltage was set to 4.5 kV in negative mode. The flow rate was set to 360 µL h^{-1} with a nebulizer gas pressure of 14.5 psi. 200 transients in a scanning range of 92 to 2000 Da were co-added for each sample, 8 megaword datasets were collected with a transient length of 2.8 s. An in-house reference material extracted using the same SPE methods from North Equatorial Pacific Intermediate Water (NEqPIW, (Green et al., 2014)), was analyzed under the same conditions, 18 times, in between environmental samples, to control for instrument variability.

Assignment of molecular formulas to detected masses was performed by two different methods based on the determination of the accurate mass in magnitude-mode spectra (MAG), or using absorption-mode processed (AMP) spectra and a connections network of predefined homologous series mass differences (Supplemental Figure S1). Phase correction and absorption-mode processing can improve the resolving power and the signal-to-noise ratio compared to conventional magnitude-mode processing without extra cost in instrumentation (Kilgour et al., 2013).

For the MAG processing, mass spectra were internally recalibrated, manually, using a list of >50 molecular formulas in a mass range of 225 to 621 expected to be in all samples. Masslists were exported from Bruker Data Analysis and then processed with the freely available ICBM-OCEAN online tool (Merder et al., 2020). Detected masses were then matched across all samples and molecular formulas assigned to this mass list, by accurate mass alone, allowing a mass error of 0.5 ppm. Maximum elemental composition ranges were $C_{3\text{-}58}H_{3\text{-}119}O_{1\text{-}32}N_{0\text{-}4}S_{0\text{-}2}P_{0\text{-}1}$, in a mass range of 92 to 1000 Da, with O/C <1.2. Unlikely elemental compositions, with >3 heteroelements (except N_3 and N_4), were removed. Additionally, 49 peaks, accounting for on average 3.5% of the total sample intensities in the environmental samples, were visually identified as contaminants with unusually high intensity introduced during sample processing and were removed from all results before data analysis. To decrease the effect of instrument variability and artifacts in formula assignment, we further chose the same minimum intensity for this detection limit, after normalization (to the sum of peaks per spectrum), for all samples (finding smallest peak per sample, the maximum of these minima was used as a new detection limit and all values below this set to 0). All molecular formulae occurring less than twice over the whole dataset were

removed. In total, 8624 molecular formulas were assigned by this method. A subset of (MAG), restricted to the mass range of *m/z* 111 to 800, and without any P-containing formulas, was used for comparison with the AMP results; this subset contained 7860 molecular formulas.

For AMP processing, mass spectra were phase corrected absorption-mode processed using AutoVectis (Spectroswiss Sárl, Lausanne, Switzerland). Here, spectra were phase corrected and presented in absorption mode (2 zero pads, second order phase correction function, "DPAK mode", F=0.5, (Kilgour and Van Orden, 2015)). Next, peaks were picked in absorption mode, with the peak detection threshold set at S/N=1.75, using the AutoPiquer algorithm (Kilgour et al., 2017) tool built in to AutoVectis. For formula assignment, connected "inference" networks of peaks separated by the repeat unit masses of common homologous series (CH_2, H_2, OH_2, OH_{-2}, NH, $H_{-1}N_{-1}O$, $H_{-2}N$, ^{13}C and $C_4O_{-1}S_{-1}$) were constructed using the AutoLogis complex organic matter assignment tool in AutoVectis. A single "seed" peak was assigned using both the accurate mass and the isotopic fine structure visible in the spectrum, using the tool for this in AutoLogis: in this study, the seed peak *m/z* 395.134759 ($C_{19}H_{23}O_9^-$ - corresponding to $C_{19}H_{23}O_9E_1$ in the syntax used by AutoLogis) was used for all spectra. The formulas of other peaks in the spectra were then automatically assigned by AutoLogis, by following the various homologous series through the inference network constructed earlier. Anomalous assignments, with errors exceeding approximately 0.5 ppm, were visually identified in a *m/z* versus mass error plot and cut from the peaklist, and the remaining formula assignments used for a third-order recalibration. The dataset was shortened as described above for the MAG dataset regarding the removal of contaminant, singletons and doubletons, and the setting of a new minimum detection limit. Maximum elemental compositions were $C_{4\text{-}40}H_{4\text{-}58}O_{1\text{-}18}N_{0\text{-}4}S_{0\text{-}2}P_{0\text{-}1}$ in a mass range of 111 to 800 Da, the total number of assigned molecular formulas was 8821.

For both datasets (MAG) and (AMP), each sample was normalized to the sum of FT-ICR-MS signal intensities. The modified aromaticity index (AI_{mod}, (Koch and Dittmar, 2006; Koch and Dittmar, 2016)), double bond equivalents (DBE, (Koch et al., 2005)), molar elemental ratios as well as the nominal and average oxidation states of carbon (NOSC, (LaRowe and Van Cappellen, 2011) were calculated for each formula and provided as averages weighted by peak intensity per sample. Additionally, molecular formulas were grouped into four descriptive compound classes with subcategories, including aromatic (AI_{mod} >0.5), highly unsaturated (AI_{mod}≤0.5 & H/C<1.5),

unsaturated (H/C≥1.5 & DBE<>0), and saturated (DBE=0) molecular formulas. All four categories were subdivided into high (O/C ≥ 0.5) and low-oxygen (O/C < 0.5) content formulas. The assignment of a formula to a compound class is ambiguous because the grouping does not consider all possible isomers. It, however, can provide likely structures and has previously been applied to identify biogeochemical DOM processing in the environment and incubation studies (Kim et al., 2006; Rivas-Ubach et al., 2018). Indices, including the degradation index I_{deg} (Flerus et al., 2012), the lability index MLB_w (D'Andrilli et al., 2015) and the "island of stability" (IOS, (Lechtenfeld et al., 2014)), and the proportion of carboxylic-rich alicyclic molecules (CRAM-like, (Chen et al., 2014; Hertkorn et al., 2006)) were calculated.

Station map and section plots were done with Ocean Data View Version 4.7.8 (Schlitzer, 2018), seafloor was added as station bottom depth in grey, interpolations used DIVA gridding. Statistical analysis were performed using R (Version 3.5.3) with the vegan package (2.5.6, Oksanen et al. (2019)).

Results

Molecular formula attribution to ultrahigh-resolution mass spectrometry data

We found an overall high agreement between FT-ICR-MS datasets processed using magnitude-mode (MAG) and absorption-mode (AMP) approaches. Our final datasets included a lower number of molecular formula assignments in MAG (n=7860) compared to AMP (n=8821) when considering the same mass range and elemental attribution, as well as the post-processing steps described above. Da Silva et al. (2020) could also assign more peaks in AMP compared to MAG in a riverine sample reference sample when selecting the signal-to-noise ratio to result in a similar number of peaks before the formula assignment step. Our analysis was, however, not focused on detailed differences within one sample but rather including post-assignment steps such as setting similar detection thresholds that we deem necessary for a meaningful interpretation of a high number of samples covering a large environmental gradient. Based on molecular formula counts, 77% of molecular formulas of AMP and 87% of MAG were shared between the results of the two workflows. When taking into account relative peak intensities, on average more than 98.5% of the total relative peak intensity was covered by the shared molecular formulas in both MAG and AMP datasets, denoting that differences are due to very small peaks.

Only 112 detected masses received different formula attributions depending on the processing. As these peaks accounted for about 1.5% of the total sample intensities and no pattern emerged, these formula assignments were removed statistical analyses. However, this finding demands further investigation in the future. Overall, the error in ppm showed a wider spread in MAG as each sample was recalibrated after formula assignment in the AMP processing pipeline (Figure 2A, Supplemental Figure S2). Formulas exclusively assigned in MAG were distributed quite evenly between descriptive compound categories, whereas formulas exclusive to AMP were dominated by (highly) unsaturated and saturated formulas. A higher frequency of nitrogen- and sulfur-containing compounds was observed in unique AMP assignments, unique peaks were not mainly attributed to the CHO class as described previously ((Da Silva et al., 2020), Figure 2B).

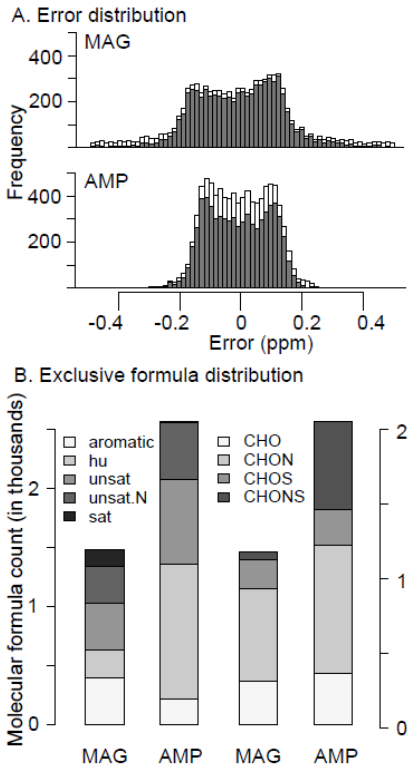

Figure 2 - Figure 2 - Comparison of MAG and AMP formula attributions. (A) Frequency of error distributions with white bars representing all molecular formulas of the respective processing and dark bars representing shared molecular formulas. (B) Exclusive formulas of MAG and AMP by compound category (aromatic, hu = highly unsaturated, unsat = unsaturated, unsat.N = unsaturated N-containing, sat = saturated) or class (CHO, CHON, CHOS, CHONS). See methods section for details.

No peaks could reliably be assigned to phosphorus-containing molecular formulas using AutoVectis/AutoLogis. This was because all such assignments produced anomalous patterns of combinations of *m/z*, signal-to-noise ratio, and mass error, indicating that these assignments were low confidence, and therefore were discounted from the inference network. As no clear pattern for P-containing molecular formulas emerged in the MAG dataset either, we have omitted this element from further data processing.

As overall patterns described throughout this study (indices, elemental ratios, multivariate analyses) were highly similar between both processing approaches, we conclude that both methods successfully detect the main trends in large datasets covering ocean basins. The AMP dataset was chosen for further data evaluation as the mass error of molecular formula assignments was lower, and their total number was higher.

Hydrographic features and bulk organic matter properties across the South Pacific

Salinities were above 36 in the upper 150 m of the eastern central waters, between stations 5 and 7 (Fig. 3A). Antarctic Intermediate Water (AAIW) was detected, with low salinity < 34.4, up to 1300 m depth in the western South Pacific (Kawabe and Fujio, 2010; Talley et al., 2011). Water temperatures were above 20°C in all surface gyre waters, denoted by salinities >34.9, between 90 and 125°W (Fig 3A,B). The sharp decrease in salinity in the surface waters west of station 10 marked the boundary between the oligotrophic SPG and the mesotrophic waters, south of the South Pacific Subtropical Front. In the mesotrophic western waters, surface biomass was greatest, with fluorescence-derived chlorophyll *a* concentrations exceeding 1 μg L^{-1} in the upper 70 m at station 13 (Fig 3D), while the chlorophyll maximum deepened to ~200 m in the central gyre waters, between stations 4 and 9. Low oxygen concentration/high AOU are introduced with waters from the oxygen minimum zone off Chile, in the eastern South Pacific (Silva et al., 2009). A relative oxygen maximum, in the dense waters >3000 m water depth in the west, points to the presence of Lower Circumpolar Deep water (LCDW) (Fig. 3C).

TDN was depleted in surface waters along the transect, with lowest values found within the limits of the 34.9 isohaline (Fig. 3G). A sharp increase in TDN concentration with depth in the east was likely due to the extension of the Peru/Chile upwelling, bringing nutrient-rich waters closer to the surface, with active respiration leading to lower oxygen concentrations. DON was higher in all surface waters (sigma-theta<26.5, DON=4.5±1.4) compared to deeper water depths (sigma-theta>26.5, DON=3.1±1.4). Solid-phase extractable nitrogen (SPE-DON, Fig 3H) showed a similar picture, but with a slight decrease in the transition zone between Eastern and Western Central Waters, and a less pronounced difference over depth between basins. SPE-DON concentrations related to chlorophyll *a* fluorescence in the Western South Pacific surface waters but did not follow the deep chlorophyll maximum (DCM) observed to deepen to almost 200 m in the central SPG.

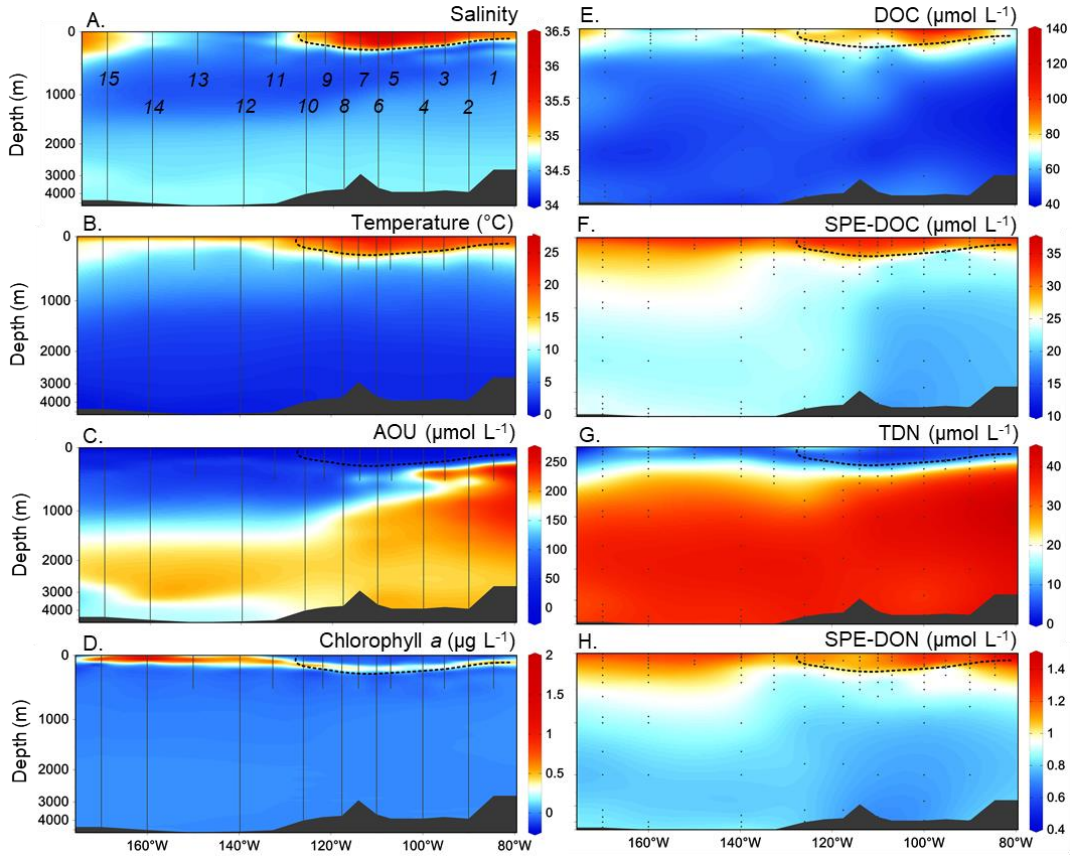

Figure 3 - Oceanographic and bulk DOM properties along cruise track. Salinity (A), temperature (B), oxygen (C), chlorophyll a concentration derived from fluorescence (D, calculated) are from CTD profiles at 1 m resolution (Zielinski et al., 2018), DOC (E), SPE-DOC (F), TDN (G) and SPE-DON (H) from discrete samples (dots on vertical lines). Numbers in panel A are station numbers, dashed line defines 34.9 isohaline denoting surface gyre waters east of 150°W; gray shaded area denotes station bottom depth. Section plots produced with Ocean Data View (Schlitzer, 2018).

DOC concentrations were generally below 115 µmol L^{-1}, with only 4 sampling points exceeding this value (Stations 2 and 4, <40 m water depth, Fig. 3E). The highest DOC concentrations were found above the 34.9 isohaline, denoting surface gyre waters (Talley et al., 2011), especially east of ~110°W. DOC concentrations were uniformly low in the deep waters. High concentrations of SPE-DOC (Fig. 3F), were not limited to the central gyre waters of highest salinity and temperature but were present in all surface waters limited by the salinity isoline. At depth, a slight accumulation of SPE-DOC was observed in the Eastern South Pacific. . In order to better understand the differential behavior of the respective DOC pools (bulk vs. PPL- SPE-DOC), we performed multiple linear regression analyses of DOC and SPE-DOC concentrations with apparent oxygen utilization (AOU), potential temperature and salinity (Table 1). The smaller slope value of SPE-DOC/AOU compared to DOC/AOU denotes a lower contribution of the extractable DOM fraction to the oxygen demand. The slope SPE-DOC/AOU does not change much when

potential temperature and salinity are introduced as model term in addition to AOU, showing that SPE-DOC can be used to differentiate water masses of contrasting ageing.

DOM molecular composition

On average, 4501±183 molecular formulas (count±SD) were detected per sample. Of these, 2098 formulas were present in all 136 samples, contributing 47±2% of the molecular formulas and 85±1% of the relative intensity per sample. Formulas shared between all samples plotted closely in van Krevelen space, while the others occupied a wider range of O/C and H/C ratios (Supplemental Figure S3). DOM molecular formula richness (number of molecular formulas per sample) was highest in the surface waters and lowest in the low-oxygen regions near the Chilean coast (Figure 4A). Weighted mean mass was 395±7 Da and similar throughout the transect, with no emerging trend but slightly more variable than the average value calculated for the reference DOM from North Equatorial Intermediate Water NEqPIW analyzed 18 times with the environmental samples (NEqPIW = 428±3 Da). Elemental ratios in the South Pacific were on average O/C = 0.41±0.01 (NEqPIW = 0.44±0.01), H/C = 1.30±0.01 (NEqPIW = 1.27±0.00), N/C = 0.023±0.002 (NEqPIW = 0.023±0.000) and S/C = 0.0014±0.0004 (NEqPIW = 0.0018±0.0002). Together, these narrow ranges illustrate the extremely high SPE-DOM compositional similarity over large geographic scales.

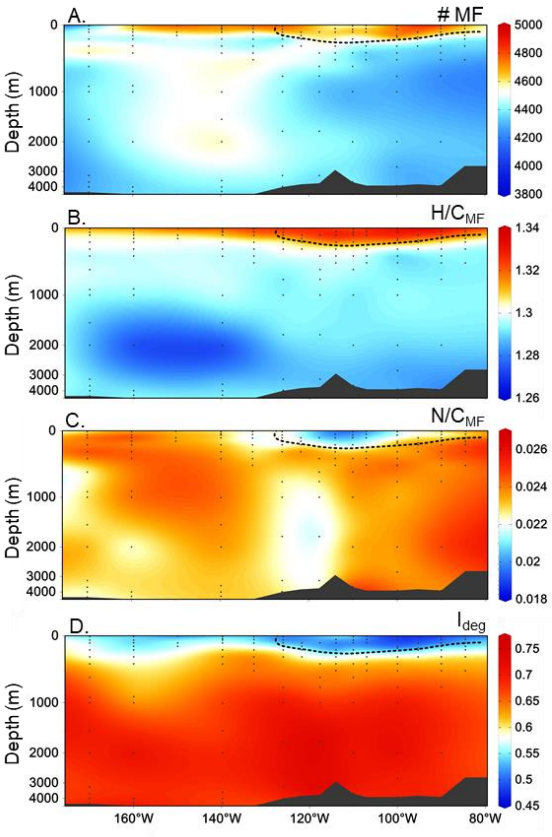

Figure 4 - DOM molecular properties from FT-ICR-MS analysis. Number of assigned formulas (A), degradation index Ideg (B) and intensity weighted elemental ratios H/C and N/C (C,D). Ideg was calculated after Flerus et al. (2012). Dashed line defines 34.9 isohaline denoting surface gyre waters east of 150°W. Dots on vertical lines are discrete sampling points. Section plots produced with Ocean Data View (Schlitzer, 2018).

In spite of the overall high similarity, clear gradients in DOM molecular composition were detected with depths and distance to coast. Molar H/C ratios were increased in the surface waters, indicating more saturated, aliphatic molecules (Figure 4C). Nitrogen was strikingly

depleted compared to carbon only in the very central gyre waters (Figure 4D), while higher N/C ratios where observed in the Western South Pacific, down to ~2000 m depth, and deeper in the east. S/C ratios were high in all surface and central deep waters and decreased below the thermocline at the easternmost stations (station 1 to 4) and in the west at station 15 below the thermocline; possible mechanisms behind this distribution could not be derived from current literature.

Calculated indices proposed to indicate susceptibility to or state of degradation generally distinguished surface from deep waters and were highly correlated in the expected directions (Table 2). The degradation index I_{deg}, which uses the relative abundances of 10 molecular formulas (Flerus et al., 2012), indicated a younger DOM signature in all South Pacific surface waters and especially in the gyre (Figure 4B). The contribution of molecular formulas to the "island of stability" (IOS, n=446, (Lechtenfeld et al., 2014)) generally correlated to the degradation index, but showed a more patchy distribution. Relative intensity-weighted contribution to the IOS (15.1±1.3%), was much lower than previously reported for the Atlantic and Southern Ocean, where more than 50% of the relative intensity were assigned to this group of presumably highly refractory molecular formulas. This difference is likely due to the different data processing as Lechtenfeld et al. (2014) used a different mass range (200-600 Da) and formula assignment criteria. The lability index, describing the relative intensity contribution of molecular formulas with H/C>1.5 (D'Andrilli et al., 2015) showed a percentage of molecular formulas thought of as more labile in DOM of up to 15% in surface waters, and a strong negative correlation to the degradation index (Table 2).

A linear regression of AOU and Ideg, similar to the regression of DOC and SPE-DOC with AOU described above, revealed a high correlation (Table 3) and a smaller slope compared to North Atlantic and the Mediterranean Sea.

TDNS concentrations were higher in the surface waters (250 to 353 nM L^{-1}, 10 m depth) and decreased with depth to less than 34 nM L^{-1} at 300 m (Supplemental Figure S4). Concentrations near the surface of station 6 were slightly elevated compared to stations 2 and 8. TDNS composition was similar between the three stations and the dominant monosaccharides were galactose, xylose, and glucose. The contribution of TDNS to DOC decreased with water

depth similar to TDNS concentrations, but was below 1.4 % at station 2 and below 2.2 % for stations 6 and 8. FDNS were always below 42 nm L^{-1} and below 2 % of TDNS (data not shown).

Discussion

Basin-scale diagenetic processing of DOM

Across ocean basins, upwelling and nutrient inputs from land increase auto- and heterotrophic DOC production in coastal areas, whereas heterotrophic utilization during water mass transport, and ageing in deeper water layers influence longitudinal distributions. Surface DOC concentrations exceeding deep ocean values are prevalent in most oceanic basins, due to photosynthetic production in the warmer, sunlit surface waters (Hansell et al., 2009) similar to those previously reported for the South Pacific Ocean (e.g. (Druffel and Griffin, 2015; Raimbault et al., 2008)).

Along the SO245 transect across the South Pacific, DOC concentrations showed a strong vertical and weaker longitudinal variability. Bulk DOC and SPE-DOC concentrations were moderately positively related ($r = 0.64$, $p<0.001$, $n=103$). Comparing the coefficient of variation for SPE-DOC (CV=0.12) to bulk DOC (CV=0.19), we find that the variability of SPE-DOC is 63% that of the bulk DOC. Especially in the surface and mesopelagic regions, increased DOC concentrations are not representatively captured by the SPE method (Supplemental Figure S5). Much of this variability of carbon concentrations is controlled by biological production and utilization. AOU reflects all respiratory processes that have taken place within a water mass since its last contact with the atmosphere, and its relationship with DOC concentration can thus reveal DOC reactivity and processing (Ogura, 1970). The DOC/AOU relationship of the entire water column is of limited value as it combines water depth where the relationship is strong with areas where the relationship is weak (Doval and Hansell, 2000). Weak relationships, for example, occur when primary production oxygen is present or sinking particulate organic matter contributes to AOU especially in deep waters (Calleja et al., 2019; Menzel, 1970). Further separation into smaller subsets along depth isopycnals was not feasible in this study due to the low number of available samples, but a first comparison of DOC and SPE-DOC/AOU nonetheless offers some insights. A decrease in the slope DOC/AOU when potential temperature is included in the multiple regression indicates that the contribution of DOC to AOU is overestimated as water mass mixing is ignored.

Values are similar to those found by Doval and Hansell (2000) for a meridional transect in the South Pacific, but water mass mixing has a greater impact in this zonal transect. The small slope of SPE-DOC/AOU and thus the small contribution to the oxygen demand is consistent with the preferential retention of refractory DOM by SPE (Arellano et al., 2018; Hansman et al., 2015; Raeke et al., 2016). Little change occurs in the SPE-DOC/AOU relationship when potential temperature and salinity are introduced as a model term in addition to AOU. SPE-DOC would thus be a good water mass tracer which allows to differentiate water masses of contrasting ageing (Igarza et al., 2019) but not water mass ageing during mixing. Interpreting the slopes of SPE-DOC/AOU and DOC/AOU in light of each other is, however, difficult as we do not know the relationship between reactivity and concentration. This relationship is unlikely to be linear as indicated by global distributions of DOC concentrations and their proposed reactivity (Hansell, 2013) or DOC degradation in controlled experiments (Osterholz et al., 2015; Shen and Benner, 2018).

Together, the lower variability of SPE-DOC concentrations compared to bulk DOC and the high similarity of DOM fingerprints support the assumption that the DOM fraction assessed via FT-ICR-MS analysis of SPE-DOM captures the more refractory component of marine DOM, while specific subgroups such as the molecular formulas used for the calculation of the I_{deg} capture DOM degradation processes. This conclusion is consistent with the findings by Hansman et al. (2015) for the Atlantic Ocean. Thus, even though SPE-DOC does not capture the whole gradient of variability within bulk DOC as shown above, its molecular analysis can still provide information on compositional changes otherwise not accessible. Previous studies have shown a strong positive correlation between AOU and the degradation index I_{deg} proposed by (Flerus et al., 2012) in the meso- and bathypelagic waters of the North Atlantic (Hansman et al., 2015) and the Mediterranean Sea (Martinez-Perez et al., 2017). We found that for the South Pacific, the slope of the regression was lower than for the North Atlantic. This denotes a lower degradation ratio per oxygen consumption unit for the South Pacific compared to the Atlantic, both ratios much lower than determined for the Mediterranean Sea (Table 3). The I_{deg} to AOU relation as well as the absolute I_{deg} only partially reflect the DOC radiocarbon ages determined for the ocean basins. The radiocarbon age for DOC in the deep South Pacific varies between 4000 and 6400 years (Druffel and Griffin, 2015), which is higher than that of the deep Sargasso Sea (4100 years, (Bauer

et al., 1992)), consistent with the decreased slope of I_{deg}/AOU. The Mediterranean Sea, on the other hand, has a DOC radiocarbon age of 4500 to 5100 years (Santinelli et al., 2015). DOC ages higher than determined for the North Atlantic render the Mediterranean Sea a unique case and emphasize a decoupling of radiocarbon age and calculated molecular degradation state. Following the approach of Martinez-Perez et al. (2017), we calculated the ratio of the standard deviation of the residuals of a linear regression model of I_{deg} with potential temperature (denoting variability caused by mixing only) and standard deviation of I_{deg}. We infer that 35% of the observed variability of the I_{deg} are not associated to water mass mixing alone. This value is lower than reported for the Mediterranean Sea (54%, (Martinez-Perez et al., 2017)), where microbial DOM degradation is enhanced due to higher water temperatures. The higher contribution of microbial DOM degradation to the I_{deg} in the Mediterranean Sea, in conjunction with fact that the faster degradation of DOM is reflected in composition of the SPE-DOC pool as high slope of I_{deg}/AOU, is consistent with findings by (Lønborg et al., 2018), who demonstrate a high temperature dependence of refractory DOM degradation, but a small difference between Atlantic and Pacific ocean basins.

Accumulation of DOM in the SPG

Bulk DOC concentrations were increased in the surface gyre waters along the zonal transect through the South Pacific. Our results are in line with observations by Raimbault et al. (2008) for the South Pacific, as well as e.g. Hansell et al. (2009) or Goldberg et al. (2010) for North Pacific and the Atlantic subtropical gyres. The discrepancy between bulk DOC and SPE-DOC concentrations observed in our study suggests a change in DOM quality between gyre and non-gyre surface waters. Here, we examine potential accumulation mechanisms based on our findings on the quality of the accumulated DOM.

Photochemical transformations of DOM

In the clear waters of the studied region, extraordinarily low concentrations of chromophoric DOM (CDOM, (Claustre and Maritorena, 2003; Swan et al., 2009) were observed previously. The authors attribute the low CDOM concentrations in the central SPG to extreme photobleaching, due to the multi-year residence times and high solar irradiation in the subtropics. Further, SAMW

(Subantarctic Mode Water) and AAIW transport photobleached material from their formation region below the gyre, thus hindering supply from CDOM-richer deep waters (Sloyan and Kamenkovich, 2007; Swan et al., 2009). The biogeochemical impact of photochemical processing of DOM is a topic of debate: irradiation partially or completely remineralizes DOM, targeting the molecules that microbes struggle to degrade. Photoinduced transformations or breakdown of molecules can render the DOM pool more recalcitrant or more labile to microbial uptake, or have no influence at all (reviewed in Mopper et al. (2015)), with most studies reporting a positive effect on bioavailability of photo-processed DOM. On the other hand, high solar irradiation can affect bacterial growth and even in high-light environments such as the South Pacific or the Mediterranean Sea, the majority of bacterial isolates showed some effect of UV-B irradiation (Matallana-Surget et al., 2012). Reintjes et al. (2019) report low cellular abundances in the surface gyre waters with $3.9x10^5$ cells mL^{-1} with the AGEAN169 marine group being especially abundant in the top 20 m in the central waters. This might, in contrast to the less abundant *Prochlorococcus*, indicate an adaptation to the low nutrient conditions, and likely also to the high irradiance regime.

We found aromatic molecular formulas depleted in the surface waters and especially the central gyre waters above the 1% PAR depth, as shown by decreased AI_{mod} and DBE compared to the deeper waters (Figure 5A,B). As aromatic compounds are prone to photochemical degradation (Stubbins and Dittmar, 2015; Stubbins et al., 2008), this process is likely the main driver of the observed distribution. The relative contributions of the molecular formula classes of highly unsaturated oxygen-poor, and to some extet the aromatic molecular formulas, follow this trend. Of the molecular formulas identified as photo-produced/-labile/-resistant during an incubation experiment with North Atlantic Deep Water (NADW)(Stubbins and Dittmar, 2015), we identified

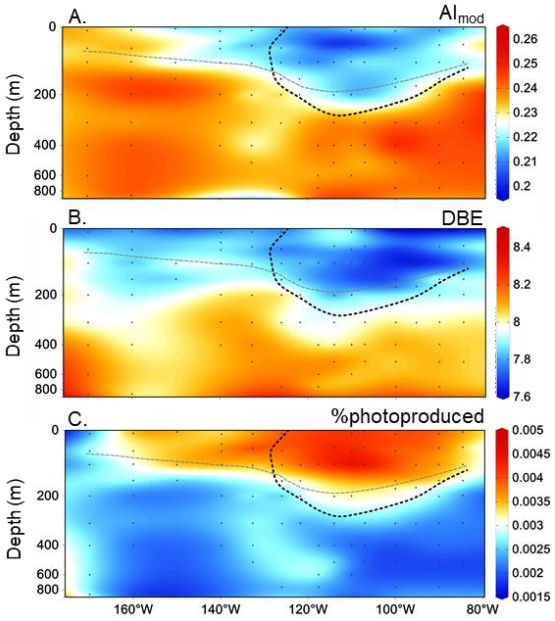

Figure 5 - Photochemical imprint on DOM molecular composition. Aromaticity index AImod (A), double-bond equivalent DBE (B) and the proportion of photo-produced molecular formulas. Dashed line defines 34.9 isohaline denoting surface gyre waters east of 150°W, gray dashed line approximates 1% PAR depth, dots on vertical lines denote discrete samples. Section plots produced with Ocean Data View (Schlitzer, 2018).

69%, 78% and 92% of the respective formulas in our dataset. Comparing the relative intensity contributions of these molecular formulas, we found that the photo-produced fraction was overall low (0.06±0.004% of total peak intensity per sample) but doubled in the surface gyre waters (Figure 5C). No horizontal or vertical trends were observed for photo-resistant or photo-labile molecular formulas, which accounted for 8.0±0.002 and 0.003±0.001 % of total peak intensity per sample (Stubbins and Dittmar, 2015). It is possible that photodegradation of different parent molecules, specific to different ocean basins, can lead to formation of similar products. Photo-induced remineralization of aromatic DOM may lead to a subsequent stimulation of bacterial growth through the production of small, labile compounds which would in turn result in a decrease in DOC concentration as well as to an increase in cell numbers, which was not observed here. Some production and accumulation of recalcitrant compounds not preferably utilized by microbes is thus likely to occur in the sunlit SPG surface, but with its low contribution to the DOM pool presumably does not constitute the sole reason for the observed DOC accumulation in the SPG.

Nutrient limitation

The SPG surface waters comprise the most oligotrophic region of the global ocean. Nitrogen, phosphate, and dissolved iron have been shown to limit primary production and heterotrophic growth in different areas of the South Pacific, where N_2 fixation by microorganisms is an important source of fixed N species. Low, but persistent N_2 fixation has been reported for the Eastern Tropical South Pacific (ETSP)(Knapp et al., 2016) and the SPG (Bonnet et al., 2008; Halm et al., 2012; Shiozaki et al., 2018) with little dust Fe input, contrasting reports of extremely high rates in the Western Tropical South Pacific (Bonnet et al., 2017). Despite low rates, the light isotopic signal in suspended particulate organic matter in the SPG suggests N_2 fixation as a dominant source of nitrogen to phytoplankton.

While all nutrients (nitrate, nitrite, phosphate, silicate) were depleted within the surface South Pacific, the South Pacific Gyre was severely nitrogen limited (Ferdelman et al., 2019a). NOx concentrations were depleted to < 1 nM resulting in N/P ratios of 1.5±2.5 in the gyre and thus substantially lower than Redfield (16/1). DOM was overall depleted in N, exhibiting bulk DON/DOC ratios around 0.051±0.022 in the core of the SPG (Redfield N/C=0.15). Molar ratios

calculated for methanol extracts and relative intensities of FT-ICR-MS molecular formulas N/C_{SPE} and N/C_{MF} (Figure 4) showed pronounced minima, especially between stations 5 to 9. Potentially labile compounds contributing to MLB_w (H/C>1.5, (D'Andrilli et al., 2015)) comprised up to 12% of the relative intensity in the surface waters. Unexpectedly, the relative contribution of these formulas was significantly higher in the central gyre waters compared to other surface waters (Supplemental Table S2). Separating the contributions to MLB_w into CHO and CHON-containing molecular formulas, we found the relative contribution of CHON labile formulas to increase by a factor of ~4 from deep to surface waters, while CHO formulas increase by a factor of only ~2.5. This indicated that the DON fraction assessed on molecular level in this study is small and significantly lower in the central gyre surface waters, but does not appear to be particularly recalcitrant. Consequently, either the index does not adequately represent the lability of the surface SPG DOM pool, or the limitation through other essential nutrients or trace metals, or photoinhibition, hinder the uptake of the DOM through the resident microbial community. Including all water depths, N/C_{bulk} ratios (0.057±0.020) were not correlated to N/C_{SPE} or N/C_{MF} ratios, but N/C_{SPE} (0.037±0.003) and N/C_{MF} (0.023±0.001) ratios were moderately related (R^2=0.53, p<0.001). Bulk C/N values (18.5±6.6), for better comparability, were roughly within the range reported by (Raimbault et al., 2008), but C/N_{SPE} (26.8±1.9) and C/N_{MF} (49.1±3.1) values were overall higher. Evidently, PPL extraction and subsequent FT-ICR-MS analysis do not capture the whole DON pool (Green et al., 2014) but likely representatively capture the basin-scale distribution of a fraction of DON. Small, rapidly cycled molecules such as free amino acids, urea or amines make up only a small portion of the DON pool, while protein amino acids, carbohydrate N and the degradation resistant nonhydrolyzable amide N have been shown to compose major fractions of the high molecular weight (HMW) DOM pool (Aluwihare et al., 2005; McCarthy et al., 1997). Letscher et al. (2015) show little use of DOC but no detectable use of DON by the upper mesopelagic SPG bacterial community, providing evidence for the existence of a recalcitrant DON pool. Both, small reactive and recalcitrant HMW moieties would not be captured efficiently with our SPE method and/or not be amenable to negative electrospray ionization in FT-ICR-MS analysis.

Accumulation of in-situ produced C-rich DOM in the closed ecosystem of the SPG (Raimbault et al., 2008), together with preferential utilization of CHON over CHO DOM

compounds by algae and bacteria to meet their nitrogen demands (Berman and Bronk, 2003) contribute to the N depletion in the SPG also observed in this study. We hypothesize that the DON pool consists of at least three reactivity fractions, with the extractable DON assessed in this study placed at intermediate reactivity in between labile, low-molecular weight compounds, and the HMWDOM pool of limited reactivity but likely making up the largest proportion, in terms of concentration.

Microbial community interactions

Disentangling the relationship between microbial producers and consumers and the dissolved organic matter pool is a fundamental step towards a better understanding of biogeochemical cycles in aquatic environments. Correlations between bacterial or phytoplankton community composition and DOM concentration or molecular composition have been shown in previous studies (Judd et al., 2006; Kujawinski et al., 2016; Li et al., 2018; Liu et al., 2020; Osterholz et al., 2016a; Osterholz et al., 2016b; Tanentzap et al., 2019). However, direct environmental evidence is scarce and the role of external drivers affecting both the living and dissolved chemical components of the system needs to be taken into account as well (Fasching et al., 2016; Kellerman et al., 2014).

Molecular formula-based diversity assessed as richness (number of molecular formulas) was higher in surface than deep waters of the South Pacific but, unlike DOC and TDN concentrations and molar ratios (N/C, H/C), not markedly different between eastern and western surface waters (Supplemental Table S1). Bacterial cell counts are lower in the central gyre compared to other surface waters, with a community composition similar to other oceanic gyres and dominated by the clades *Prochlorococcus*, SAR11, SAR116, SAR86, and the AEGEAN-169 marine group (Reintjes et al., 2019). DOM molecular composition and diversity assessed via molecular formula counts and the Shannon Wiener index did not correlate to total cell counts (n=108), nor to bacterial community composition and diversity derived from fluorescence in-situ hybridization FISH (n=73) or sequencing (n=45). It is to note that relative abundance of a bacterial clade does not necessarily reflect its activity (Campbell et al., 2011). It has further been shown that members of the same clade can have different metabolic capabilities, and different

microbes may well be able to perform the same roles in the environment (Gomez-Consarnau et al., 2012; Mou et al., 2008).

Potentially labile molecular formulas are expected to show strongest relationships to bacterial utilization. However, weak correlations with relative abundances of bacterial clades SAR 11 ($r = -0.39$, $p<0.05$), SAR86 ($r = -0.31$, $p<0.05$), SAR202 ($r = 0.48$, $p<0.001$), SAR324 ($r = 0.36$, $p<0.01$) and SAR406 ($r = 0.32$ $p<0.01$) were observed in our study. No relationship between the labile fraction ($H/C>1.5$) or nitrogen content of DOM could be established to *Prochlorococcus* abundance as might have been expected from its function as the most abundant phototrophic producer in the ecosystem (Flombaum et al., 2013; Reintjes et al., 2019). These examples illustrate the difficulty of disentangling the mixed signal of production and degradation in DOM fingerprints over large spatial scales in an environment often thought of as extreme in terms of nutrient availability, irradiation and water clarity - but quite homogenous regarding DOM molecular composition.

Conclusion

Distribution of DOC concentrations across the South Pacific indicates slow microbial degradation and a considerable DOC accumulation in the central gyre surface waters. The highly similar molecular fingerprint reflected photochemical reworking and preferential utilization of DOM-N. Unexpected were the high similarity to surface water DOM outside the gyre and a high potential lability of the accumulated material. Our first assessment of the molecular-level composition of central gyre DOM provides new insights into potential mechanisms behind the accumulation of DOM in surface gyre waters. A clearer delineation of mixing versus degradation signals, as well as potentially a DOM-source specific lability assessment, in the molecular formula-level information provided by ultrahigh resolution mass spectrometry needs to be targeted in the future.

Acknowledgements

We are most grateful to Captain L. Mallon, the crew and scientific party of SO245 who made work on board a great experience. We thank I. Ulber and M. Friebe (DOC/TDN quantification), K. Klaproth (FT-ICR-MS), and R. Weinert (carbohydrates) for help in the laboratory. X. Anton Alvarez-Salgado provided helpful comments on earlier versions of the manuscript. The UltraPac Expedition SO245 was funded by the Federal Ministry of Education and Research of Germany (Grant 03G0245A).

Conflict of Interest

The authors declare that the research was conducted in the absence of any commercial or financial relationships that could be construed as a potential conflict of interest.

References

Aluwihare, L.I., Repeta, D.J., Pantoja, S. and Johnson, C.G., 2005. Two chemically distinct pools of organic nitrogen accumulate in the ocean. Science, 308(5724): 1007-10.

Arellano, A.R., Bianchi, T.S., Hutchings, J.A., Shields, M.R. and Cui, X., 2018. Differential effects of solid-phase extraction resins on the measurement of dissolved lignin-phenols and organic matter composition in natural waters. Limnology and Oceanography: Methods, 16(1): 22-34.

Arrieta, J.M. et al., 2015. Dilution limits dissolved organic carbon utilization in the deep ocean. Science.

Bauer, J.E., Williams, P.M. and Druffel, E.R.M., 1992. 14C activity of dissolved organic carbon fractions in the north-central Pacific and Sargasso Sea. Nature, 357(6380): 667-670.

Benner, R. and Biddanda, B., 1998. Photochemical transformations of surface and deep marine dissolved organic matter: Effects on bacterial growth. Limnology and Oceanography, 43(6): 1373-1378.

Berman, T. and Bronk, D.A., 2003. Dissolved organic nitrogen: A dynamic participant in aquatic ecosystems. Aquatic Microbial Ecology, 31(3): 279-305.

Biersmith, A. and Benner, R., 1998. Carbohydrates in phytoplankton and freshly produced dissolved organic matter. Marine Chemistry, 63(1–2): 131-144.

Bonnet, S., Caffin, M., Berthelot, H. and Moutin, T., 2017. Hot spot of N₂ fixation in the western tropical South Pacific pleads for a spatial decoupling between N₂ fixation and denitrification. Proceedings of the National Academy of Sciences, 114(14): E2800-E2801.

Bonnet, S. et al., 2008. Nutrient limitation of primary productivity in the Southeast Pacific (BIOSOPE cruise). Biogeosciences, 5(1): 215-225.

Calleja, M.L., Al-Otaibi, N. and Morán, X.A.G., 2019. Dissolved organic carbon contribution to oxygen respiration in the central Red Sea. Scientific Reports, 9(1): 4690.

Campbell, B.J., Yu, L.Y., Heidelberg, J.F. and Kirchman, D.L., 2011. Activity of abundant and rare bacteria in a coastal ocean. Proceedings of the National Academy of Sciences of the United States of America, 108(31): 12776-12781.

Carlson, C. and Ducklow, H., 1995. Dissolved organic carbon in the upper ocean of the central equatorial Pacific Ocean, 1992: Daily and finescale vertical variations. Deep Sea Res II, 42: 639-656.

Chen, H. et al., 2014. Ultrahigh resolution mass spectrometric differentiation of dissolved organic matter isolated by coupled reverse osmosis-electrodialysis from various major oceanic water masses. Marine Chemistry, 164(0): 48-59.

Claustre, H. and Maritorena, S., 2003. The Many Shades of Ocean Blue. Science, 302(5650): 1514-1515.

Claustre, H., Sciandra, A. and Vaulot, D., 2008. Introduction to the special section bio-optical and biogeochemical conditions in the South East Pacific in late 2004: the BIOSOPE program. Biogeosciences, 5(3): 679-691.

Comisarow, M.B. and Marshall, A.G., 1974. Fourier transform ion cyclotron resonance spectroscopy. Chemical Physics Letters, 25(2): 282-283.

D'Andrilli, J., Cooper, W.T., Foreman, C.M. and Marshall, A.G., 2015. An ultrahigh-resolution mass spectrometry index to estimate natural organic matter lability. Rapid Commun Mass Spectrom, 29(24): 2385-401.

Da Silva, M.P., Kaesler, J.M., Reemtsma, T. and Lechtenfeld, O.J., 2020. Absorption Mode Spectral Processing Improves Data Quality of Natural Organic Matter Analysis by Fourier-Transform Ion Cyclotron Resonance Mass Spectrometry. Journal of the American Society for Mass Spectrometry, 31(7): 1615-1618.

Dandonneau, Y., Montel, Y., Blanchot, J., Giraudeau, J. and Neveux, J., 2006. Temporal variability in phytoplankton pigments, picoplankton and coccolithophores along a transect through the North Atlantic and tropical southwestern Pacific. Deep Sea Research Part I: Oceanographic Research Papers, 53(4): 689-712.

Dittmar, T., 2014. Reasons behind long-term stability of dissolved organic matter. In: D.A. Hansell and C.A. Carlson (Editors), The Biogeochemistry of Marine Dissolved Organic Matter. Academic Press.

Dittmar, T., Koch, B., Hertkorn, N. and Kattner, G., 2008. A simple and efficient method for the solid-phase extraction of dissolved organic matter (SPE-DOM) from seawater. Limnology and Oceanography-Methods, 6: 230-235.

Doval, M.D. and Hansell, D.A., 2000. Organic carbon and apparent oxygen utilization in the western South Pacific and the central Indian Oceans. Marine Chemistry, 68(3): 249-264.

Druffel, E.R.M. and Griffin, S., 2015. Radiocarbon in dissolved organic carbon of the South Pacific Ocean. Geophysical Research Letters, 42(10): 4096-4101.

Fasching, C., Ulseth, A.J., Schelker, J., Steniczka, G. and Battin, T.J., 2016. Hydrology controls dissolved organic matter export and composition in an Alpine stream and its hyporheic zone. Limnology and Oceanography, 61(2): 558-571.

Ferdelman, T.G., Klockgether, G., Downes, P. and Lavik, G., 2019a. Nutrient Data from CTD Nisken Bottles from Sonne Expedition SO-245 "UltraPac". PANGAEA.

Ferdelman, T.G. et al., 2019b. Calibrated Dissolved O2 Data from RV Sonne Expedition SO245 "UltraPac". PANGAEA.

Flerus, R. et al., 2012. A molecular perspective on the ageing of marine dissolved organic matter. Biogeosciences, 9(6): 1935-1955.

Flombaum, P. et al., 2013. Present and future global distributions of the marine Cyanobacteria Prochlorococcus and Synechococcus. Proceedings of the National Academy of Sciences, 110(24): 9824.

G. Marshall, A. et al., 2013. Mass Resolution and Mass Accuracy: How Much Is Enough? Mass Spectrometry, 2(Spec Iss): S0009.

Goldberg, S.J., Carlson, C.A., Bock, B., Nelson, N.B. and Siegel, D.A., 2010. Meridional variability in dissolved organic matter stocks and diagenetic state within the euphotic and mesopelagic zone of the North Atlantic subtropical gyre. Marine Chemistry, 119(1–4): 9-21.

Gomez-Consarnau, L., Lindh, M.V., Gasol, J.M. and Pinhassi, J., 2012. Structuring of bacterioplankton communities by specific dissolved organic carbon compounds. Environmental Microbiology, 14(9): 2361-78.

Graeber, D. et al., 2012. Technical Note: Comparison between a direct and the standard, indirect method for dissolved organic nitrogen determination in freshwater environments with high dissolved inorganic nitrogen concentrations. Biogeosciences, 9(11): 4873-4884.

Green, N.W. et al., 2014. An intercomparison of three methods for the large-scale isolation of oceanic dissolved organic matter. Marine Chemistry, 161: 14-19.

Gruber, N., 2008. Chapter 1 - The Marine Nitrogen Cycle: Overview and Challenges. In: D.G. Capone, D.A. Bronk, M.R. Mulholland and E.J. Carpenter (Editors), Nitrogen in the Marine Environment (Second Edition). Academic Press, San Diego, pp. 1-50.

Halm, H. et al., 2012. Heterotrophic organisms dominate nitrogen fixation in the South Pacific Gyre. ISME J, 6(6): 1238-49.

Hansell, D.A., 2013. Recalcitrant Dissolved Organic Carbon Fractions. Annual Review of Marine Science, 5(1): 421-445.

Hansell, D.A. and Carlson, C.A., 1998. Deep-ocean gradients in the concentration of dissolved organic carbon. Nature, 395(6699): 263-266.

Hansell, D.A., Carlson, C.A., Repeta, D.J. and Schlitzer, R., 2009. Dissolved organic matter in the ocean - a controversy stimulates new insights. Oceanography, 22(4): 202-211.

Hansman, R.L., Dittmar, T. and Herndl, G.J., 2015. Conservation of dissolved organic matter molecular composition during mixing of the deep water masses of the northeast Atlantic Ocean. Marine Chemistry(0).

Hertkorn, N. et al., 2006. Characterization of a major refractory component of marine dissolved organic matter. Geochimica Et Cosmochimica Acta, 70(12): 2990-3010.

Igarza, M., Dittmar, T., Graco, M. and Niggemann, J., 2019. Dissolved Organic Matter Cycling in the Coastal Upwelling System Off Central Peru During an “El Niño” Year. Frontiers in Marine Science, 6(198).

Jiao, N. et al., 2011. The microbial carbon pump and the oceanic recalcitrant dissolved organic matter pool. Nat Rev Micro, 9(7): 555-555.

Jørgensen, L., Lechtenfeld, O.J., Benner, R., Middelboe, M. and Stedmon, C.A., 2014. Production and transformation of dissolved neutral sugars and amino acids by bacteria in seawater. Biogeosciences, 11(19): 5349-5363.

Judd, K.E., Crump, B.C. and Kling, G.W., 2006. Variation in dissolved organic matter controls bacterial production and community composition. Ecology, 87(8): 2068-79.

Karl, D.M., 2002. Nutrient dynamics in the deep blue sea. Trends in Microbiology, 10(9): 410-8.

Kawabe, M. and Fujio, S., 2010. Pacific ocean circulation based on observation. Journal of Oceanography, 66(3): 389-403.

Kellerman, A.M., Dittmar, T., Kothawala, D.N. and Tranvik, L.J., 2014. Chemodiversity of dissolved organic matter in lakes driven by climate and hydrology. Nat Commun, 5.

Kilgour, D.P.A. et al., 2017. Autopiquer - a Robust and Reliable Peak Detection Algorithm for Mass Spectrometry. Journal of The American Society for Mass Spectrometry, 28(2): 253-262.

Kilgour, D.P.A. and Van Orden, S.L., 2015. Absorption mode Fourier transform mass spectrometry with no baseline correction using a novel asymmetric apodization function. Rapid Communications in Mass Spectrometry, 29(11): 1009-1018.

Kilgour, D.P.A., Wills, R., Qi, Y. and O'Connor, P.B., 2013. Autophaser: An Algorithm for Automated Generation of Absorption Mode Spectra for FT-ICR MS. Analytical Chemistry, 85(8): 3903-3911.

Kim, S., Kaplan, L.A. and Hatcher, P.G., 2006. Biodegradable Dissolved Organic Matter in a Temperate and a Tropical Stream Determined from Ultra-High Resolution Mass Spectrometry. Limnology and Oceanography, 51(2): 1054-1063.

Kind, T. and Fiehn, O., 2007. Seven Golden Rules for heuristic filtering of molecular formulas obtained by accurate mass spectrometry. BMC Bioinformatics, 8(105): 1471-2105.

Knapp, A.N., Casciotti, K.L., Berelson, W.M., Prokopenko, M.G. and Capone, D.G., 2016. Low rates of nitrogen fixation in eastern tropical South Pacific surface waters. Proceedings of the National Academy of Sciences, 113(16): 4398-4403.

Koch, B.P. and Dittmar, T., 2006. From mass to structure: an aromaticity index for high-resolution mass data of natural organic matter. Rapid Communications in Mass Spectrometry, 20(5): 926-932.

Koch, B.P. and Dittmar, T., 2016. From mass to structure: an aromaticity index for high-resolution mass data of natural organic matter. Rapid Communications in Mass Spectrometry, 30(1): 250-250.

Koch, B.P., Witt, M.R., Engbrodt, R., Dittmar, T. and Kattner, G., 2005. Molecular formulae of marine and terrigenous dissolved organic matter detected by electrospray ionization Fourier transform ion cyclotron resonance mass spectrometry. Geochimica Et Cosmochimica Acta, 69(13): 3299-3308.

Kujawinski, E.B., Longnecker, K., Barott, K.L., Weber, R.J.M. and Kido Soule, M.C., 2016. Microbial Community Structure Affects Marine Dissolved Organic Matter Composition. Frontiers in Marine Science, 3(45).

Landa, M. et al., 2018. Major changes in the composition of a Southern Ocean bacterial community in response to diatom-derived dissolved organic matter. FEMS Microbiology Ecology, 94(4).

LaRowe, D.E. and Van Cappellen, P., 2011. Degradation of natural organic matter: A thermodynamic analysis. Geochimica et Cosmochimica Acta, 75(8): 2030-2042.

Lechtenfeld, O.J. et al., 2014. Molecular transformation and degradation of refractory dissolved organic matter in the Atlantic and Southern Ocean. Geochimica Et Cosmochimica Acta, 126(0): 321-337.

Letscher, R.T. et al., 2015. Microbial community composition and nitrogen availability influence DOC remineralization in the South Pacific Gyre. Marine Chemistry(0).

Letscher, R.T. and Moore, J.K., 2015. Preferential remineralization of dissolved organic phosphorus and non-Redfield DOM dynamics in the global ocean: Impacts on marine productivity, nitrogen fixation, and carbon export. Global Biogeochemical Cycles, 29(3): 325-340.

Li, H.-Y. et al., 2018. The chemodiversity of paddy soil dissolved organic matter correlates with microbial community at continental scales. Microbiome, 6(1): 187.

Liu, S. et al., 2020. Different carboxyl-rich alicyclic molecules proxy compounds select distinct bacterioplankton for oxidation of dissolved organic matter in the mesopelagic Sargasso Sea. Limnology and Oceanography, n/a(n/a).

Lønborg, C., Álvarez–Salgado, X.A., Letscher, R.T. and Hansell, D.A., 2018. Large Stimulation of Recalcitrant Dissolved Organic Carbon Degradation by Increasing Ocean Temperatures. Frontiers in Marine Science, 4(436).

Marshall, A.G., Hendrickson, C.L. and Jackson, G.S., 1998. Fourier transform ion cyclotron resonance mass spectrometry: A primer. Mass Spectrometry Reviews, 17(1): 1-35.

Martinez-Perez, A.M. et al., 2017. Molecular composition of dissolved organic matter in the Mediterranean Sea. Limnology and Oceanography, 62(6): 2699-2712.

Matallana-Surget, S. et al., 2012. Response to UVB radiation and oxidative stress of marine bacteria isolated from South Pacific Ocean and Mediterranean Sea. Journal of Photochemistry and Photobiology B: Biology, 117: 254-261.

McCarthy, M., Pratum, T., Hedges, J. and Benner, R., 1997. Chemical composition of dissolved organic nitrogen in the ocean. Nature, 390(6656): 150-154.

Medeiros, P.M. et al., 2016. A novel molecular approach for tracing terrigenous dissolved organic matter into the deep ocean. Global Biogeochemical Cycles, 30(5): 689-699.

Mentges, A., Feenders, C., Deutsch, C., Blasius, B. and Dittmar, T., 2019. Long-term stability of marine dissolved organic carbon emerges from a neutral network of compounds and microbes. Scientific Reports, 9(1): 17780.

Menzel, D.W., 1970. The role of in situ decomposition of organic matter on the concentration of non-conservative properties in the sea. Deep Sea Research and Oceanographic Abstracts, 17(4): 751-764.
Menzel, D.W. and Vaccaro, R.F., 1964. THE MEASUREMENT OF DISSOLVED ORGANIC AND PARTICULATE CARBON IN SEAWATER. Limnology and Oceanography, 9(1): 138-142.
Merder, J. et al., 2020. ICBM-OCEAN: Processing Ultrahigh-Resolution Mass Spectrometry Data of Complex Molecular Mixtures. Anal Chem, 92(10): 6832-6838.
Mopper, K., Kieber, D.J. and Stubbins, A., 2015. Chapter 8 - Marine Photochemistry of Organic Matter: Processes and Impacts. In: D.A. Hansell and C.A. Carlson (Editors), Biogeochemistry of Marine Dissolved Organic Matter (Second Edition). Academic Press, Boston, pp. 389-450.
Mopper, K. et al., 1992. Determination of sugars in unconcentrated seawater and other natural waters by liquid chromatography and pulsed amperometric detection. Environmental Science & Technology, 26(1): 133-138.
Morel, A. et al., 2007. Optical properties of the "clearest" natural waters. Limnology and Oceanography, 52(1): 217-229.
Mou, X.Z., Sun, S.L., Edwards, R.A., Hodson, R.E. and Moran, M.A., 2008. Bacterial carbon processing by generalist species in the coastal ocean. Nature, 451(7179): 708-U4.
Obernosterer, I. and Benner, R., 2003. Competition between biological and photochemical processes in the mineralization of dissolved organic carbon. Abstracts of Papers of the American Chemical Society, 225: 52.
Obernosterer, I., Reitner, B. and Herndl, G.J., 1999. Contrasting effects of solar radiation on dissolved organic matter and its bioavailability to marine bacterioplankton. Limnology and Oceanography, 44(7): 1645-1654.
Ogawa, H. and Ogura, N., 1992. Comparison of two methods for measuring dissolved organic carbon in sea water. Nature, 356(6371): 696-698.
Ogura, N., 1970. The relation between dissolved organic carbon and apparent oxygen utilization in the Western North Pacific. Deep Sea Research and Oceanographic Abstracts, 17(2): 221-231.
Oksanen, J. et al., 2019. vegan: Community Ecology Package. R package version 2.5-6. https://CRAN.R-project.org/package=vegan.
Osterholz, H., Kirchman, D.L., Niggemann, J. and Dittmar, T., 2016a. Environmental Drivers of Dissolved Organic Matter Molecular Composition in the Delaware Estuary. Frontiers in Earth Science, 4(95).
Osterholz, H., Niggemann, J., Giebel, H.A., Simon, M. and Dittmar, T., 2015. Inefficient microbial production of refractory dissolved organic matter in the ocean. Nat Commun, 6: 7422.
Osterholz, H. et al., 2016b. Deciphering associations between dissolved organic molecules and bacterial communities in a pelagic marine system. ISME J, 10(7): 1717-30.
Perminova, I.V. et al., 2014. Molecular Mapping of Sorbent Selectivities with Respect to Isolation of Arctic Dissolved Organic Matter as Measured by Fourier Transform Mass Spectrometry. Environmental Science & Technology, 48(13): 7461-7468.
Qi, Y. et al., 2011. Variation of the Fourier Transform Mass Spectra Phase Function with Experimental Parameters. Analytical Chemistry, 83(22): 8477-8483.
Raeke, J., Lechtenfeld, O.J., Wagner, M., Herzsprung, P. and Reemtsma, T., 2016. Selectivity of solid phase extraction of freshwater dissolved organic matter and its effect on ultrahigh resolution mass spectra. Environmental Science: Processes & Impacts, 18(7): 918-927.
Raimbault, P. and Garcia, N., 2008. Evidence for efficient regenerated production and dinitrogen fixation in nitrogen-deficient waters of the South Pacific Ocean: impact on new and export production estimates. Biogeosciences, 5(2): 323-338.
Raimbault, P., Garcia, N. and Cerutti, F., 2008. Distribution of inorganic and organic nutrients in the South Pacific Ocean − evidence for long-term accumulation of organic matter in nitrogen-depleted waters. Biogeosciences, 5(2): 281-298.
Reintjes, G. et al., 2019. On-Site Analysis of Bacterial Communities of the Ultraoligotrophic South Pacific Gyre. Applied and Environmental Microbiology, 85(14): e00184-19.
Rivas-Ubach, A. et al., 2018. Moving beyond the van Krevelen Diagram: A New Stoichiometric Approach for Compound Classification in Organisms. Analytical Chemistry, 90(10): 6152-6160.
Romera-Castillo, C., Letscher, R.T. and Hansell, D.A., 2016. New nutrients exert fundamental control on dissolved organic carbon accumulation in the surface Atlantic Ocean. Proceedings of the National Academy of Sciences, 113(38): 10497.

Santinelli, C., Follett, C., Retelletti Brogi, S., Xu, L. and Repeta, D., 2015. Carbon isotope measurements reveal unexpected cycling of dissolved organic matter in the deep Mediterranean Sea. Marine Chemistry, 177: 267-277.

Schlitzer, R., 2018. Ocean Data View. https://odv.awi.de.

Sharp, J.H. et al., 2002. Final dissolved organic carbon broad community intercalibration and preliminary use of DOC reference materials. Marine Chemistry, 77(4): 239-253.

Shen, Y. and Benner, R., 2018. Mixing it up in the ocean carbon cycle and the removal of refractory dissolved organic carbon. Scientific Reports, 8(1): 2542.

Shiozaki, T. et al., 2018. Linkage Between Dinitrogen Fixation and Primary Production in the Oligotrophic South Pacific Ocean. Global Biogeochemical Cycles, 32(7): 1028-1044.

Silva, N., Rojas, N. and Fedele, A., 2009. Water masses in the Humboldt Current System: Properties, distribution, and the nitrate deficit as a chemical water mass tracer for Equatorial Subsurface Water off Chile. Deep Sea Research Part II: Topical Studies in Oceanography, 56(16): 1004-1020.

Skoog, A. and Benner, R., 1997. Aldoses in various size fractions of marine organic matter: Implications for carbon cycling, 42. American Society of Limnology and Oceanography, Waco, TX, United States.

Sleighter, R.L. and Hatcher, P.G., 2008. Molecular characterization of dissolved organic matter (DOM) along a river to ocean transect of the lower Chesapeake Bay by ultrahigh resolution electrospray ionization Fourier transform ion cyclotron resonance mass spectrometry. Marine Chemistry, 110(3–4): 140-152.

Sloyan, B. and Kamenkovich, I., 2007. Simulation of Subantarctic Mode and Antarctic Intermediate Waters in Climate Models. Journal of Climate - J CLIMATE, 20: 5061-5080.

Smith, D.F., Podgorski, D.C., Rodgers, R.P., Blakney, G.T. and Hendrickson, C.L., 2018. 21 Tesla FT-ICR Mass Spectrometer for Ultrahigh-Resolution Analysis of Complex Organic Mixtures. Analytical Chemistry, 90(3): 2041-2047.

Stubbins, A. and Dittmar, T., 2015. Illuminating the deep: Molecular signatures of photochemical alteration of dissolved organic matter from North Atlantic Deep Water. Marine Chemistry, 177, Part 2: 318-324.

Stubbins, A. et al., 2008. Relating carbon monoxide photoproduction to dissolved organic matter functionality. Environmental Science & Technology, 42(9): 3271-3276.

Swan, C.M., Siegel, D.A., Nelson, N.B., Carlson, C.A. and Nasir, E., 2009. Biogeochemical and hydrographic controls on chromophoric dissolved organic matter distribution in the Pacific Ocean. Deep Sea Research Part I: Oceanographic Research Papers, 56(12): 2175-2192.

Talley, L.D., Pickard, G.L., Emery, W.J. and Swift, J.H., 2011. Descriptive Physical Oceanography: An Introduction. Academic Press, Elsevier Ltd.

Tanentzap, A.J. et al., 2019. Chemical and microbial diversity covary in fresh water to influence ecosystem functioning. Proceedings of the National Academy of Sciences: 201904896.

Thingstad, T.F., Hagstrom, A. and Rassoulzadegan, F., 1997. Accumulation of Degradable DOC in Surface Waters: Is it Caused by a Malfunctioning Microbial Loop? Limnology and Oceanography, 42(2): 398-404.

Van Wambeke, F. et al., 2008. Factors limiting heterotrophic bacterial production in the southern Pacific Ocean. Biogeosciences, 5(3): 833-845.

Wienhausen, G., Noriega-Ortega, B.E., Niggemann, J., Dittmar, T. and Simon, M., 2017. The Exometabolome of Two Model Strains of the Roseobacter Group: A Marketplace of Microbial Metabolites. Frontiers in Microbiology, 8(1985).

Williams, P.M. and Druffel, E.R.M., 1987. Radiocarbon in dissolved organic matter in the central North Pacific Ocean. Nature, 330(6145): 246-248.

Zielinski, O., Henkel, R., Voß, D. and Ferdelman, T.G., 2018. Physical oceanography during SONNE cruise SO245 (UltraPac). PANGAEA.